International Journal of Optics and Applications 2014, 4(2): 46-53
DOI: 10.5923/j.optics.20140402.04

Simulation and Temperature Characteristics Improvement of 1.3μm AlGaInAs Multiple Quantum Well Laser

Vahid Bahrami Yekta, Hassan Kaatuzian*

Photonics Research Laboratory (PRL), Electrical Engineering Department, Amirkabir University of Technology, Tehran, Iran

Abstract In this paper the effects of strain on the barriers of a 1.3 μm AlGaInAs-InP multiple quantum well laser are investigated by solving Kohn-Luttinger and effective mass equations. The results have shown that many enhancements can be made to the laser structure by introducing 0.2% compressive strain to the barriers. 20% improvement in mode gain-current density characteristic and 3% improvement in material gain spectra were obtained while the leakage and Auger currents reduced significantly. Energy levels in conduction and valence bands are calculated and used to simulate the material gain. The effects of temperature increase on the recombination and Auger current densities are also investigated.

Keywords AlGaInAs-InP multiple quantum well laser, Uncooled laser, Strain in barrier, Kohn-Luttinger Hamiltonian

1. Introduction

The performance of the semiconductor laser has been dramatically improved since its invention in 1962. Today it came to be indispensable for our life as optical components connecting home and the Internet as well as long-distance large-capacity trunk networks. Wavelengths used for optical communication are mainly 1.55 μm for long-distance transmission and 1.3 μm for short- and mid distance transmission due to the minimum loss and minimum dispersion in optical fiber. It is required that the band gap of the material composing semiconductor laser correspond to the oscillation wavelength of the laser and its lattice constant match to the lattice constant of the substrate to maintain high crystal quality. Typical compound semiconductors that meet these conditions are GaInAsP, AlGaInAs grown on the InP substrate and GaInNAs, (Ga)InAs dots structure grown on the GaAs substrate. Today, GaInAsP is widely used from view points of reliability of device and handling in its process. The lattice constant and the band gap of a compound semiconductor can be controlled by changing the composition of the compound. In the structure that two compound semiconductors with different band gaps pile up alternatively, electrons and holes are confined in the lower band gap layers. The thickness of the lower band gap layer approaches to electron mean free pass (several 10 nm), energy levels of electron and hole are quantized. This structure is called quantum well (QW) or multiple quantum well (MQW) when the structure consists of multiple layers. In the MQW structure, novel phenomenon which cannot be obtained in the bulk material appears. By applying MQW structure to the active region of the laser, the performances of the laser such as threshold current, temperature characteristics and modulation frequency were significantly improved and MQW became an essential technology for realizing high performance lasers.

Uncooled laser that can operate at room temperature with a stable wavelength and output power is very desirable. Commercial GaInAsP laser needs to have huge cooling system which is caused mainly by poor confinement of electrons in the conduction band due to relatively small conduction band offset ($\Delta E_c = 0.4\Delta E_g$). The effective mass of electrons in conduction band is much less than the effective mass of holes in valence band so the laser efficiency increases more with making stronger barriers for electrons rather than holes at high temperatures. Large conduction band offset up to ($\Delta E_c = 0.72\Delta E_g$) is achieved with AlGaInAs barriers and wells [1].

When a MQW system is pumped, the carriers travel in the barriers and drop in the quantum wells. The excess carriers separate the Fermi level into two quasi Fermi levels. The separation between two quasi Fermi levels depends on the pump strength. When the pump is strong enough to a separation equal to the material bandgap, the material becomes transparent for photon energies equal to the bandgap. Optical gain is achieved when the system is pumped beyond transparency condition. The differential gain is the rate that the gain increases with carrier density. It depends on how quickly the band edge carrier density can be

* Corresponding author:
hsnkato@aut.ac.ir (Hassan Kaatuzian)
Published online at http://journal.sapub.org/optics
Copyright © 2014 Scientific & Academic Publishing. All Rights Reserved

increased. The band edge carrier density can be increased by symmetric band structure ($m_c = m_v$) and steep change in density of states. Both these conditions exist in strained quantum well. Two dimensional density of state has a perfect step like shape and the effective masses can be adjusted by the strain of the well.

Strain in barriers enhances the effective mass of the injected carriers and the quantum wells are populated more efficiently as more carriers can get into the wells before recombination. This effect has been investigated and calculated in this paper. We used COMSOL Multiphysics software to solve Kohn-Luttinger Hamiltonian equations for finding valence band energy levels and single band effective mass equation to find conduction band energy levels. At first we simulated the structure that was fabricated and presented in [2], it is a MQW ridge wave guide AlGaInAs-InP laser with lattice match barriers, Then we investigated the same structure with 0.2% compressive strain and 0.2% tensile strain barriers. (see Figure 1)

In section II we introduce the theoretical model for simulating the structure. In section III we describe and discuss the simulation results and improvements. We have a conclusion section at the end.

2. Theory

2.1. Energy Levels in Conduction and Valence Bands

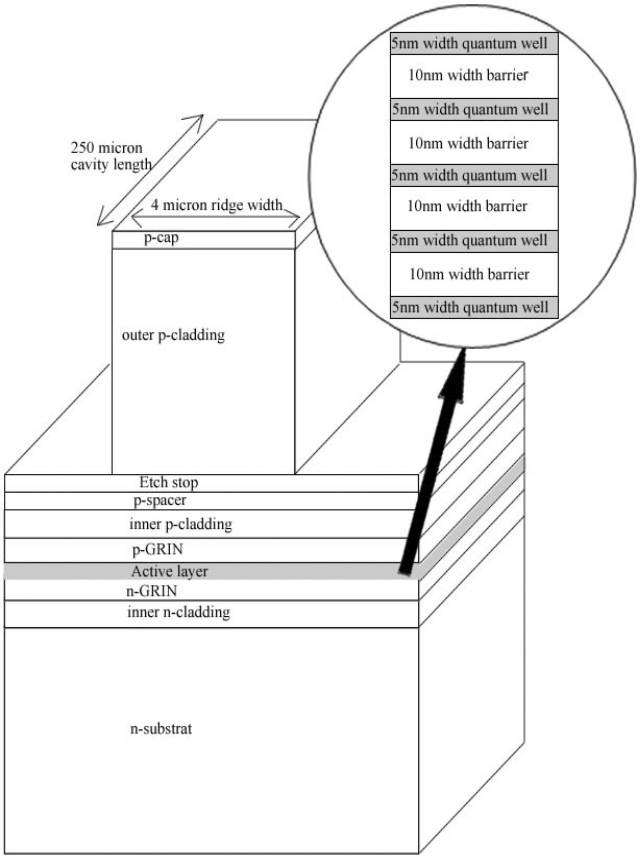

Figure 1. The ridge wave guide laser structure under study

Figure 1 shows the under study structure. It is a ridge wave guide laser diode. It has active layer with five quantum wells and four barriers between them. Two graded index layers and two spacer layers enwind the active layer.

We simulate laser structure with $Al_{0.161}Ga_{0.102}In_{0.737}As$ strained quantum wells and three different barrier compositions. First lattice match barriers with composition of $Al_{0.267}Ga_{0.203}In_{0.53}As$ as in the [2], second 0.2% compressive strain barriers with composition of $Al_{0.23}Ga_{0.203}In_{0.547}As$ and third 0.2% tensile strain barriers with composition of $Al_{0.30}Ga_{0.203}In_{0.547}As$.

The composition of graded index and spacer layers are listed in Table 1.

Table 1. The composition of layers in the under study structure

Layer	Composition	Thickness(μm)
n-substrate	InP	1.25
n transition GRIN	$Al_{0.4128}Ga_{0.0672}In_{0.52}As$ to $Al_{0.48}In_{0.52}As$	0.01
Inner n-cladding	$Al_{0.48}In_{0.52}As$	0.11
n-GRIN	$Al_{0.48}In_{0.52}As$ to $Al_{0.267}Ga_{0.203}In_{0.52}As$	0.1
Active layer	Five quantum wells: $Al_{0.161}Ga_{0.102}In_{0.737}As$ Four barriers: $Al_{0.267}Ga_{0.203}In_{0.52}As$	QW:0.005 Barriers:0.01
p-GRIN	$Al_{0.267}Ga_{0.203}In_{0.52}As$ to $Al_{0.48}In_{0.52}As$	0.1
Inner p-cladding	$Al_{0.48}In_{0.52}As$	0.11
p transition GRIN	$Al_{0.48}In_{0.52}As$ to $Al_{0.4128}Ga_{0.0672}In_{0.52}As$	0.01
p-spacer	InP	0.05
Etch stop	InGaAsP	0.025
outer p-cladding	InP	1.25
p-cap	InGaAs	0.2

To obtain conduction sub bands we solve single band effective mass equation that is used for parabolic sub bands [3]

$$\frac{-\hbar^2}{2m_c^*}\nabla^2\psi + V_c\psi = E_c\psi \qquad (1)$$

Where:

ψ : Envelope function;

$\hbar$: Planck's constant divided by 2π;

m_c^* : Electron effective mass in conduction band;

V_c : Conduction band potential;

E_c : Electron energy level in conduction band;

The strain can be compressive or tensile. According to Figure 2 we can see the effect of strain on the conduction and valence band structure in a strained quantum well.

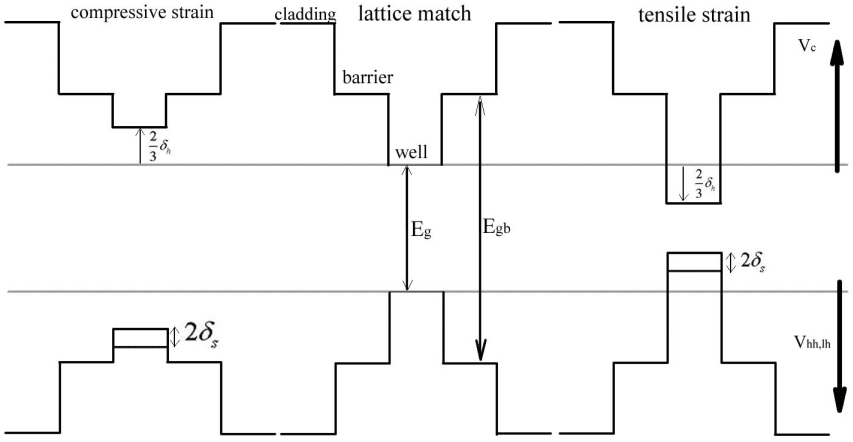

Figure 2. Effect of strain on conduction and valence bands in MQW

In Figure 2 the strain constant ε can be defined as [3]

$$\varepsilon = \frac{a_b - a_q}{a_b} \tag{2}$$

Where a_b, a_q are the barriers and quantum well lattice constants.

So the hydro static potential δ_h in Figure 2 would be [3]

$$\delta_h = 2a(1 - \frac{C_{11}}{C_{12}})\varepsilon \tag{3}$$

Where:

a: hydro static deformation potential;

C_{11}, C_{12}: Elastic stiffness constants;

The valence band structure in quantum well is not parabolic, so multi band effective mass theory is used [4] we solve the resulting coupled differential equations known as Kohn-Luttinger Hamiltonian equations for finding heavy and light holes energy levels and Envelope functions [3]

$$\begin{bmatrix} H & M & N & 0 \\ M^* & L & 0 & N \\ N^* & 0 & L & -M \\ 0 & N^* & -M^* & H \end{bmatrix} \psi = E_v \psi \tag{4}$$

$$H = \frac{-\hbar^2}{2m_0}[(k_x{}^2 + k_y{}^2)(\gamma_1 + \gamma_2) - (\gamma_1 - 2\gamma_2)\frac{\partial^2}{\partial z^2}] + V_{hh,lh} \tag{5}$$

$$L = \frac{-\hbar^2}{2m_0}[(k_x{}^2 + k_y{}^2)(\gamma_1 - \gamma_2) - (\gamma_1 + 2\gamma_2)\frac{\partial^2}{\partial z^2}] + V_{hh,lh} \tag{6}$$

$$M = \frac{i2\sqrt{3}\hbar^2}{2m_0}(-k_y - k_x)\gamma_3 \frac{\partial}{\partial z} \tag{7}$$

$$N = \frac{-\sqrt{3}\hbar^2}{2m_0}[\gamma_2(k_x{}^2 - k_y{}^2) - 2i\gamma_3 k_x k_y] \tag{8}$$

m_0: free electron mass;

$\gamma_1, \gamma_2, \gamma_3$: luttinger parameters;

k_x, k_y: Components of the transverse wave vector;

$V_{hh,lh}$: Potential of heavy and light holes in the valence band;

In Figure 2 δ_s is the shear potential and defined as follows [3]

$$\delta_s = 2b(1 + \frac{C_{11}}{C_{12}})\varepsilon \tag{9}$$

Here b is the shear deformation potential.

Any quaternary parameter Q_{abcd} that is needed for calculations of conduction and valence bands can be obtained by interpolation:

$$Q_{Al_yGa_xIn_{1-x-y}As}$$

$$_{t_xIn_{1-x-y}As} = (1-x-y)Q_{InAs} + yQ_{AlAs} + : \tag{10}$$

From the corresponding binary material parameters Q_{ij} which were extracted from [5-10].

The unstrained band gap for $Al_yGa_xIn_{1-x-y}As$ is given as [11], [12]

$$E_g(x,y) = (0.36 + 2.093y + 0.629x + 0.577y^2 + 0.436x^2 + 1.013xy - 2.0xy(1-x-y)) \text{ eV}. \tag{11}$$

The appropriate strain shifts are then added to this value.

2.2. Optical Gain and Current Models

The optical gain transition depends on the polarization and as a function of photon energy can be written as [13]

$$G(E') = \frac{q^2|MB|^2}{E'\varepsilon_0 m_0{}^2 c\hbar n_{eff} W} \cdot \sum_{i,j} \int_{E_g}^{E_{gb}} m_{r,ij} C_{i,j} A_{i,j} (f_c - f_v) L(E' - E) dE \tag{12}$$

W,q,c and n_{eff} are quantum well width ,electron charge, light vacuum speed and effective refractive index;

$|MB|^2$: Bulk momentum transition matrix element;

i,j : quantum numbers in conduction and valence band;

$C_{i,j}$: Spatial overlap factor;

$A_{i,j}$: Angular anisotropy factor;

f_c, f_y : Electron Fermi functions;

$L(E)$ is the Lorentzian line shape function that convolved with gain spectra to determine the effects of intra band transitions [14]. Each individual transition contributing to the gain continuum is itself broadened by scattering.

$$L(E'-E)=\frac{1}{\pi}\frac{\hbar/\tau_{in}}{(E'-E)^2+(\hbar/\tau_{in})^2} \quad (13)$$

Where τ_{in} is the intra band relaxation time that we choose it 0.1ps according to [2].

The carrier effective mass in the i_{th} sub band can be calculated from [5]

$$m_i^{-1}=\Gamma_q m_w^{-1}+(1-\Gamma_q)m_b^{-1} \quad (14)$$

Γ_q: confinement factor of the carrier Envelope function in the Quantum well for nth sub band;

m_w: carrier effective mass in the well that calculate by quaternary formula;

m_b: carrier effective mass in the barriers that calculate by quaternary formula;

So the reduced effective mass between i_{th} conduction sub band and j_{th} valence sub band is obtained [5]

$$m_{r,ij}^{-1}=m_i^{-1}+m_j^{-1} \quad (15)$$

The angular anisotropy factor is normalized so the angular average is unity. For TE transitions (the electric field in the plane of the QW) its relation will be [13]

$$\begin{aligned} A_{ij} &= (3/4)(1+\cos^2\theta_{ij}) \quad (\text{heavyhole}) \\ &= (1/4)(5-3.\cos^2\theta_{ij}) \quad (\text{lighthole}) \end{aligned} \quad (16)$$

For TM transitions (the electric field normal to the plane of the QW) its relation will be

$$\begin{aligned} A_{ij} &= (3/2)(\sin^2\theta_{ij}) \quad (\text{heavyhole}) \\ &= (1/2)(4-3.\sin^2\theta_{ij}) \quad (\text{lighthole}) \end{aligned} \quad (17)$$

Where the angular factor is

$$\cos^2\theta_{ij}=E_{ij}/E \quad (18)$$

Where E_{ij} is the transition energy between conduction sub band i_{th} and valence sub band j_{th}.

The bulk averaged momentum matrix element between conduction < s | and valence | x > state is:

$$|M|^2=\frac{m^2E_G(E_G+\Delta)}{6m_c(E_G+2\Delta/3)} \quad (19)$$

The occupation probability of the states in conduction and valence bands, also known as Fermi function, is as follows [15]

$$f_{c,v}(E,E_{fc,fv})=\frac{1}{1+\exp\left[\frac{(E-E_{fc,fv})}{kT}\right]} \quad (20)$$

$E_{fc,fv}$ are the quasi Fermi levels in conduction and valence bands and k is Boltzmann constant. The carrier density in a band is given by the integration over of the product of the occupation probability of the carriers and the density of states over the entire band, for non parabolic band structure the carrier density can be obtained [16], [17]

$$n=\sum_n\int_0^{+\infty}\rho(k)\left[f_c(E_{cn}(k),E_{fc})\right]dk \quad (21)$$

$$p=\sum_{HH,LH}\int_0^{+\infty}\rho(k)\left[1-f_v(E_{vn}(k),E_{fv})\right]dk \quad (22)$$

That the summation is over all states in conduction (n) and valence (HH, LH) bands.

For AlGaInAs-InP material systems the conduction band is assumed to be parabolic so the conduction band integration simplifies to [13]

$$n=\frac{m_c kT}{\pi\hbar^2 W}\sum_n \ln\left\{1+\exp\left(\frac{E_{cn}-E_{fc}}{kT}\right)\right\} \quad (23)$$

We can use these relations as recursive equations to calculate the quasi Fermi levels and Fermi probabilities. In the gain formula, the graded index layer emissions have been calculated that cause the second peak in gain spectra. We also include band gap renormalization effect in our model.

To calculate current density we just investigate two main current components in these lasers: Radiative and Auger current [13], [18]

$$\begin{aligned} J_{radiative} &= qW\frac{16\pi^2 n_{eff}q^2E|MB|^2}{\varepsilon_0 m_0^2 c^3\hbar^4 W} \\ &\cdot\sum_{i,j}\int m_{ri,j}C_{i,j}f_c(1-f_v)dE \end{aligned} \quad (24)$$

$$J_{Auger}=qWCnp^2 \quad (25)$$

Where C is the Auger recombination coefficient and n,p are carrier concentrations. The temperature dependence of C is described by [19], [20]

$$C = C_0 \exp(\frac{-\Delta E_a}{kT}) \quad (26)$$

ΔE_a is the activation energy of the Auger process and the value of 0.06 eV is used. C_0 value is obtained from [19] and is taken to be 5×10^{-29} cm^6s^{-1}, respectively.

In high temperatures leakage current density becomes important [5]

$$J_{lk} = q(v_{QW}W\frac{N_w}{\tau_w} + (d_g - v_{QW}W)\frac{N_b}{\tau_b}) \quad (27)$$

$$N_b = N_{c,b}\exp[(F_c - \Delta E_c)/k_BT] \quad (28)$$

$$N_w = N_{c,w}\exp[(F_c - \Delta E_c)/k_BT] \quad (29)$$

$N_{c,w}$: Well effective density of states in a truncated parabolic Γ conduction band;

$N_{c,b}$: regular effective density of states in the Γ conduction band of barriers;

F_c: quasi Fermi level;

ΔE_c: limit of energy levels top of the QW to count for calculation;

v_{QW}: number of QWs;

k_B: Boltzman constant;

d_g: width of guiding region;

$\tau_{w,b}$: life time of electrons above the barriers;

Peak material gain multiply by optical confinement factor will result in peak mode gain. Optical confinement factor is a portion that shows the confinement of optical mode in active region that depends on the structure of the device. For our structure, optical confinement factor is taken from [2], 0.009 respectively.

As described in [2] the mode gain-current density characteristic can be estimated by McIlroy formula (14). So using (14), we obtain mode gain-current density plots for three different barrier compositions in 25˚C and 85˚C [21].

$$G_{Modal} = \Gamma G_0[\ln(\frac{J}{J_0}) + 1] \quad (30)$$

Γ: optical confinement factor;

We can also calculate the optimum gain per quantum well with McIlroy formula [21], Total threshold gain is calculated by the fact that in threshold gain should be equal with total losses [22]

$$G_{th} = \Gamma g_{th} = \alpha_i + \alpha_m = \alpha_i + \frac{1}{2L}\ln\frac{1}{R_1R_2} \quad (31)$$

Where:

α_i: internal loss

α_m: mirror loss

L: cavity length

R_1, R_2: mirror reflectivity

By calculating the optimum gain G_0 per quantum well with McIlroy formula at the highest expected temperature and divided total threshold gain to it, we can calculate the optimum number of quantum wells.

3. Simulation and Results Discussions

Figure 3 shows the material gain-photon energy plot for three different barrier compositions ,as it is obvious the compressive strain barriers has the best gain spectra that it has more quantity in peak and the peak gain photon energy is about 0.956 eV that it is closer to 1.3μm wavelength photon energy.

The first peak gain photon energy depends on the first conduction band energy level and the first heavy hole energy level. Table 2 shows the energy levels in these three situations.

Table 2. Energy levels in conduction and valence bands for three different barrier compositions

	Lattice match barriers	0.2% tensile	0.2% compressive
1st CB	0.1396	0.1478	0.1247
1st HH	0.00258	0.003988	-0.00002
1st LH	0.1031	0.1105	0.0923

The compressive strain barrier has the lowest conduction band energy level, which shows the better electron confinement the first heavy hole level is almost zero and has a negligible effect on transition energy. The first light hole level has more change so the graded index peak become closer to the Quantum Well gain peak [23].

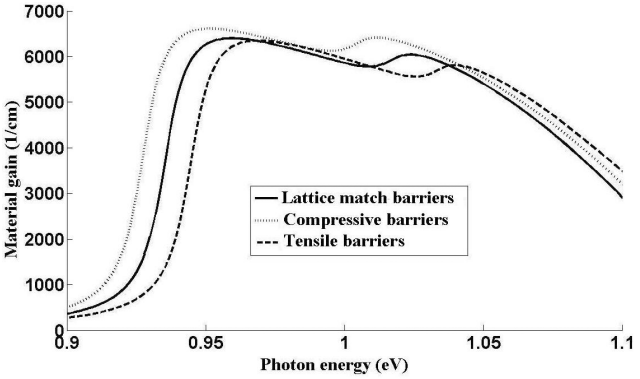

Figure 3. Material gain Vs photon energy for different barrier strains

Figure.4 shows Auger current density-carrier density plots in 25˚C and 85˚C. Auger current density increases sharply with temperature and cause degradation in internal efficiency has a direct effect on the threshold and increase it.

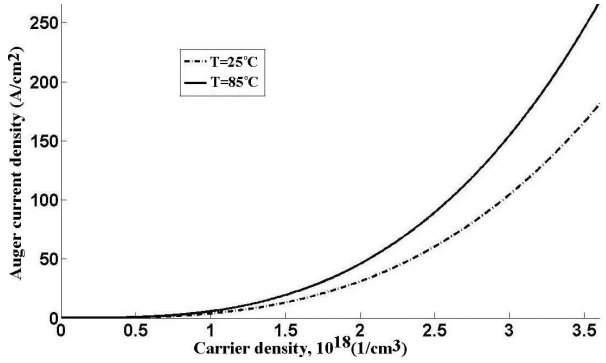

Figure 4. Auger current density-carrier density characteristic in different temperatures

Figure 5 shows Radiative current density-carrier density plots in 25˚C and 85˚C, the Radiative current density decreases with temperature and causes internal efficiency to degrade. The compressive strain barrier has the lowest Radiative current density, because of its quasi Fermi level. As the strain changes from tensile to compressive the conduction band quasi Fermi level become lower and valence band quasi Fermi level become higher proportional to the band edge. The Radiative current density depends on Fermi probability function in conduction band, lower quasi Fermi level in conduction band decreases the Fermi probability function and result in reduction in Radiative current density. The valence band quasi Fermi level acts in the same manner.

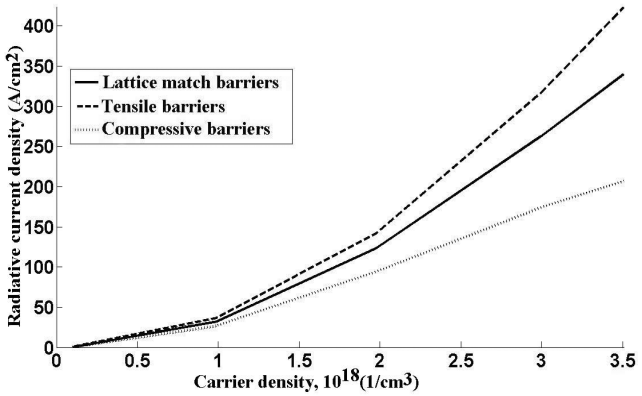

(a)

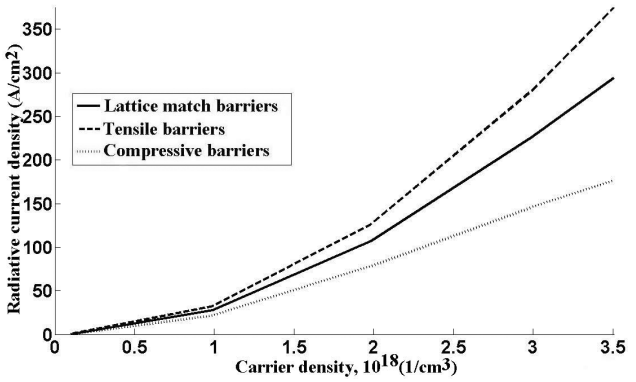

(b)

Figure 5. Radiative current density-carrier density. (a)T=25˚C. (b) T=85˚C

Figure 6 shows leakage current density-carrier density characteristic. In low carrier densities leakage current is negligible but in high temperatures, the laser structure needs high carrier density to reach threshold so leakage current become important. As it is obvious from Figure 6, compressive strain barriers have the lowest leakage current due to better confinement of electrons and lower Fermi levels.

We obtain material gain-carrier density plots in 25˚C and 85˚C (see Figure 7). That can be use for interpreting the transparency [24]. These plots can be approximated by [15]

$$g = g_0 \ln\left(\frac{N}{N_{tr}}\right) \tag{32}$$

In this approximation N is the carrier density, N_{tr} is the transparency carrier density and g_0 is the gain coefficient.

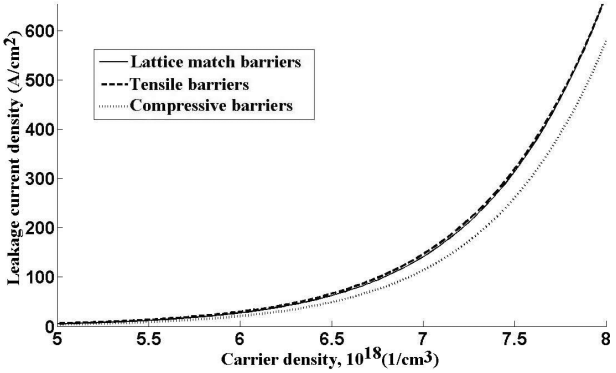

(a)

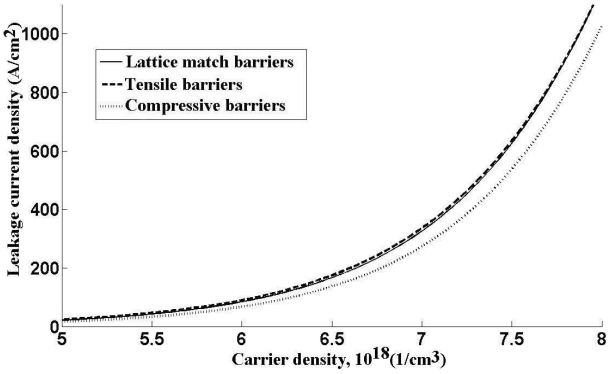

(b)

Figure 6. Leakage current density-carrier density. (a) T=25˚C. (b) T=85˚C

The transparency occurs when the difference between quasi Fermi levels reaches to band gap energy [5]. From transparency, the McIlroy threshold can be obtained. The differential gain is the derivation of gain from (32) is calculated as [15]

$$\frac{\partial g}{\partial N} = \frac{g_0}{N_{tr}} \tag{33}$$

High differential gain is essential for high speed modulation that obtains from low transparency carrier density. So to obtain low transparency carrier density the quantum well has to be designed in such a way that there exists a density of states as low as possible and a closely matched density of states in the valence and conduction band [25], [26].

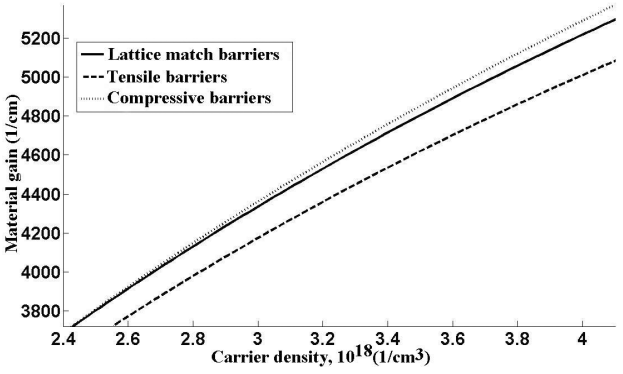

(a)

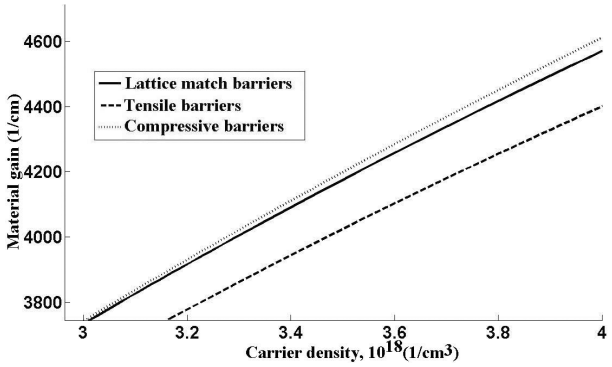

(b)

Figure 7. Material gain-carrier density. (a) T=25˚C. (b) T=85˚C

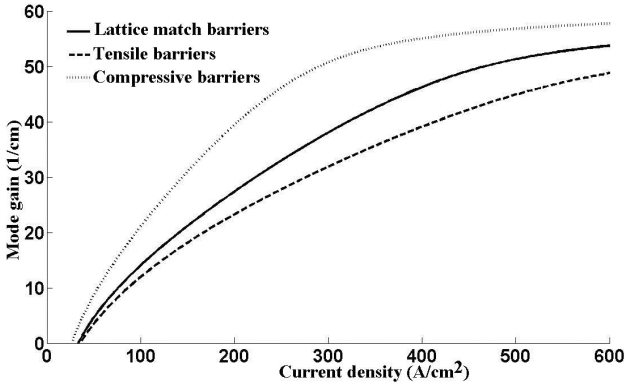

(a)

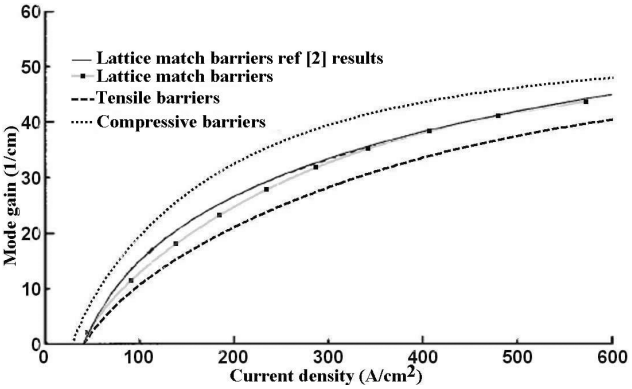

(b)

Figure 8. Mode gain-current density. (a) T=25˚C. (b) T=85˚C

Figure 8 shows the mode gain-current density characteristic in 25˚C and 85˚C. In the lattice match barrier case in 85˚C our results have good agreement with [2] results. The compressive strain barrier mode gain plot shows significant improvement, about 20% proportional to lattice match case.

4. Conclusions

In summary we have presented the background theory for optical gain and current density simulation of strained multiple quantum well lasers. We applied this theory to 1.3μm laser structure that was fabricated and presented in [2] with three different barrier compositions. In the lattice match barriers case simulations, good agreements have been obtained in comparison with results reported in [2]. For the first time we showed 0.2% compressive strain barriers in multiple quantum wells can make 20% improvement in mode gain-current density characteristic and 3% improvement in material gain spectra. Also Radiative, Auger and leakage current densities have been reduced significantly at higher temperature 85˚C.

ACKNOWLEDGMENTS

We would like to thank the Research Deputy of Amirkabir University of Technology for the research grant support. Also we thank Mr. Mohammad Sedghi for his role in editing and submission procedure of this paper.

REFERENCES

[1] Y. G. Zhang, J. X. Chen, Y. Q. Chen, M. Qi, A. Z. Li, K. Fröjdh, B. stoltz, J. Cryst. Growth 227 (2001) 329.

[2] S. R. Selmic, T. M. Chou, J. P. Sih, J. B. Kirk, A. Mantie, J. K. Butler, D. Bour, G.A.Evans "Design and Characterization of 1.3-μm AlGaInAs–InP Multiple-Quantum Well Lasers" IEEE JOURNAL ON SELECTED TOPICS IN QUANTUM ELECTRONICS, VOL.7, NO.2, 2001pp. 16-19.

[3] S. L. Chuang, "Efficient band-structure calculations of strained quantum wells," Phys. Rev. B, vol.43, no.12, pp.9649–9661, Apr. 1991.

[4] D. A. Borido and L. J. Sham, "Effective masses of holes at GaAs-Al-GaAs heterojunction," Phys. Rev. B., vol. 31, pp. 888–892, 1985.

[5] P. S. Zory, Quantum Well Lasers. San Diego, CA: Academic, 1993, pp. 58–150.

[6] G. P. Agrawal and N. K. Dutta, Semiconductor Lasers. New York: Van Norstrand Reinhold, 1993, pp. 30–135.

[7] W. W. Chow, S. W. Koch, and M. Sargent, III, Semiconductor Laser Physics. New York: Springer-Verlag, 1994, pp. 35–205.

[8] C. G. Van de Walle, "Band lineups and deformational potentials in the model solid theory," Phys. Rev. B, vol. 39, no. 3, pp. 1871–1883, 1989.

[9] S. Adachi, "Material parameters of InGaAsP and related binaries," J. Appl. Phys., vol. 53, no. 12, pp. 8775–8793, 1982.

[10] J. Minch, S. H. Park, T. Keating, and S. L. Chuang, "Theory and Experiment of InGaAsP and InGaAlAs Long-Waveleng th Strained Quantum-Well Lasers," IEEE J. Quantum Electron., vol. 35, pp.771–782, 1999.

[11] Y.K Kuo, S.H Yen a, M.W Yao , M.L Chen, B.T Liou Numerical study on gain and optical properties of AlGaInAs,InGaNAs, and InGaAsP material systems for 1.3-µm semiconductor lasers ,optics communications, 2007.

[12] J.C.L.Yong, J.M.Rorison, I.H.White, "1.3-µm Quantum Well InGaAsP, AlGaInAs and InGaAsN Laser Material Gain:A Theoretical Study," IEEE J. Quantum Electron., vol. 38, pp.1553–1564, 2002.

[13] S. R. Chinn, P. S. Zory, and A. R. Reisinger, "A model for GRIN SCH-SQW diode lasers," IEEE J. Quantum Electron., vol. 24, pp.2191–2213, 1988.

[14] A. I. Kucharska and D. J. Robbins, "Lifetime broadening in GaAs-Al-GaAs quantum well lasers," IEEE. J. Quantum Electron., vol. 26, pp.443–448, 1990.

[15] L.A.Coldren and S.W.Corzin, Diode Lasers and Photonic Integrated Circuits. New York: Wiley-Interscience, 1995.

[16] D.Ahn,S.L.Chaung and Y.C.Chang ,"Valence Band Mixing Effects on the Gain and Refractive Index Change of quantum well lasers," J. Appl. Phys., vol. 64, pp. 4056–4064, 1988.

[17] U. Menzel, A. Barwolff, D. Ackermann, R. Puchert and M. Voss, "Modeling the Temperature Dependence of Threshold current External Differential Efficiency and Lasing Wavelength in Qw Laser Diode," Semicond.Sci.Technol, vol10, pp.1382-1392, 1995.

[18] J.W.Pan and J.I.Chyi, "theoretical study of the temperature dependence of 1.3-µm AlGaInAs–InP Multiple-Quantum Well Lasers," IEEE J. Quantum Electron., vol. 32, pp.2133–2138, 1996.

[19] S.Seki, H.Oohashi, H.Sugiura, T.Hirono and K.Yokoyama, "Study on the dominant mechanisms for the temperature sensitivity of threshold current in 1.3-µm InP-based strained layer Quantum Well Lasers," IEEE J. Quantum Electron., vol. 32, pp.1478–1486, 1996.

[20] M.C.Wang, K.Kash, C.E.Za, R.Bhat and S.L.Chaung, "Measurement of nonradiative recombination rates in strained layer Quantum Well systems," Appl. Phys.Lett, vol. 62, pp. 166–168, 1993.

[21] P. W. McIlroy, A. Kurobe, and Y. Uematsu, "Analysis and application of theoretical gain curves to the design of multi-quantum-well lasers," IEEE. J. Quantum Electron. vol. 21, pp. 1958–1963, 1985.

[22] H.Kaatuzian, Photonics vol.1, 3'rd edition, AKU press 2012, pp.110-157.

[23] V.Bahrami Yekta, H.Kaatuzian, "A Novel Investigation on Using Strain in Barriers of 1.3 µm AlGaInAs-InP Uncooled Multiple Quantum Well Lasers", Commun. Theor. Phys. 54 529, 2010.

[24] T.C Peng, Y.Huang, C.Yang, K.Huang, F.Lee, C.Hu, M.Wu, and C.Ho "Low-Cost and High-Performance 1.3-AlGaInAs–InP Uncooled Laser Diodes," IEEE PHOTONICS TECHNOLOGY LETTERS, VOL. 18, NO. 12, JUNE 15, 2006.

[25] E. Yabnolovitch and E. O. Kane "band-structure engineering of Semiconductor Lasers for optical communications," J.Lightwave Technol., vol.6, pp.1292–1299, 1988.

[26] B. Zhao and A. yariv, "Quantum Well Semiconductor Lasers," in Semiconductor Lasers l: fundamentals, E.Kapon, Ed San Diego CA: Academic, 1999.